Nonlinear Dyn (2022) 108:4231–4242
https://doi.org/10.1007/s11071-022-07379-6

ORIGINAL PAPER

Transient dynamics in electronic neuron-like circuits in application to modeling epileptic seizures

Nikita M. Egorov · Danil D. Kulminskiy · Ilya V. Sysoev · Vladimir I. Ponomarenko · Marina V. Sysoeva

Received: 9 November 2021 / Accepted: 15 March 2022 / Published online: 26 March 2022

Abstract In complex systems like neural circuits, transient dynamics can stay of a large interest, being a promising explanation of the observed biological phenomena. In particular, spike-wave discharges (SWDs, the main encephalographic manifestation of absence seizures) were recently considered as possible long transient processes, since signal analysis showed no special mechanism of their termination while a number of initiation mechanisms were described in the literature. Here, we construct the ensemble of eight mesoscale models (electronic circuits) different by connectivity matrix and show that they indeed demonstrate long quasiregular transient dynamics in a reasonable area of parameters. All models from the ensemble were networks consisting of 14 electronic FitzHugh–Nagumo neuron oscillators connected based on anatomical laws for thalamocortical system. Most of networks were able to demonstrate epiletiform-like activity of reasonable duration in response to short in time external driving which is one of known mechanisms for absence epilepsy. The distribution of model SWDs by length was comparable with what is known for animal models. The proposed models are of fundamental interest being first known electronic model of absence seizures. They can be also used for testing and validating approaches for directed connectivity analysis which are very essential in brain study.

Keywords Electrical neuron-like circuit · Thalamocortical brain network · Epileptiform activity · FitzHugh–Nagumo model

N. M. Egorov · D. D. Kulminskiy · I. V. Sysoev (✉) · V. I. Ponomarenko · M. V. Sysoeva
Saratov Branch of the Kotel'nikov Institute of Radioengineering and Electronics of Russian Academy of Sciences, 38, Zelyonaya str., Saratov, Russia 410019
e-mail: ivssci@gmail.com

N. M. Egorov · M. V. Sysoeva
Yuri Gagarin State Technical University of Saratov, 77, Politekhnicheskaya str., Saratov, Russia 410054

D. D. Kulminskiy
Sirius University of Science and Technology, 1 Olympic Ave, Sochi, Russia 354340

I. V. Sysoev · V. I. Ponomarenko
Saratov State University, 83, Astrakhanskaya str., Saratov, Russia 410012

1 Introduction

Traditionally, study of biological systems takes a number of steps: the first observation of a phenomenon, setting an experiment to detect and reproduce it with reasonable confidence, measurement of experimental data and data analysis to study the phenomenon quantitatively, synthesis of mathematical models. For spike-wave discharges (encephalographic manifestation of absence epilepsy see [1]), all these steps have been mostly performed for today; the main results are available in the reviews [1–5] and some others.

Constructing models in a form of electronic circuits is a next significant step, when testing the ideas and outcomes achieved from experimental data anal-

ysis and mathematical modeling for validity. First of all, radioengineering experiment allows to test models for robustness, to detect whether the models are not fragile, whether the desired regimes modeling experimental data exist not in a very narrow, experimentally inaccessible area of parameters or cannot be destroyed due to imperfect and unequal elements or due to noise. Electronic circuits were multiple used previously for modeling biological systems including single neurons and their ensembles [6–8].

The work [9] showed that spike-wave discharges can be modeled as long transient processes in large (about 500 of elements) networks of mathematical neurons. The transient process initiated by an short in time external stimulus terminates by itself without any external control system, which matches the modern ideas [10]. During a transient process, the system demonstrates quasiregular oscillations with mostly constant frequency and shape. This can be explained if the system exhibits motion near a unstable periodic orbit with very slow repulsion.

To test this hypothesis, the detailed study of a simplified version of the above constructed thalamocortical system model was performed in [11]. The simplified models consisted of 14 model neurons. This investigation showed that the observed behavior can be obtained due to another mechanism: the motion takes place in the condensation of trajectories, preceding by parameter the cycle saddle-node bifurcation, when two cycles of nonzero size: one stable and one unstable appear together from this condensation [12,13]. The electronic circuit was developed for this 14-neuron model in [14] using SPICE simulation software. The simulations provided a hope that the transient dynamics observed in the mathematical model can be seen experimentally.

If the modeled behavior is typical, it should preserve at least for small variations in coupling strength and connectivity architecture. In the population of genetic animal models of absence epilepsy (WAG/Rij [1] and GAERS [2] rats), there is a large diversity in frequency and length of spike-wave discharges (SWDs) [15]—the main encephalographic manifestation of absence epilepsy. The connectivity in different animals also varies a lot [16]. Similarly, there should exist a population of network models which differ in details of couplings architecture, being able to reproduce the epileptic regimes with different appearance rate and longitude. Such a population variability for small changes in connectivity matrix can be achieved in SPICE simulation, as it was shown in [17]. Additionally, the dependency of model SWD length on the driving duration and final phase was considered. So, the works [11,14,17] provided a basis for observation of long transients in radioengineering experiment in application to modeling SWDs.

This work aims to present a first hardware realization of SWD model in a form of electronic circuit. The circuit constructed based on principles of real brain thalamocortical system is able to reproduce epileptiform activity. We also show that implementing different connectivity architectures with small difference between them it is possible to affect the model SWD duration and appearance rate, reproducing variability known from biological studies.

2 Model

2.1 Mathematical model of the thalamocortical network

The simplified version [19] of FitzHugh–Nagumo neuron model [20,21] was used for individual element of the network. There were two reasons for this. First, this version was previously realized as a electronic circuit [8] (actually, another earlier realization is also known [22], but we did not have enough elements of necessary quality to construct 14 generators of this type). Second, it is simpler to analyze. The element was linked with a simple linear coupling:

$$\begin{aligned} \varepsilon \dot{u}_i(t) &= u_i(t) - \frac{u_i^3(t)}{3} - v_i(t) + \sum_{j \neq i} k_{i,j} u_j, \\ \dot{v}_i &= u_i(t) + a_i, \end{aligned} \tag{1}$$

where $u(t)$ and $v(t)$ are variables qualitatively corresponding to transmembrane potential and activation current; ε is a time scale parameter characterizing relative rate of ion current activation/deactivation; $k_{i,j}$ are coupling coefficients; a is a bifurcation parameter determining a regime of activity of individual element, $a \in [0; 2]$. For a separate element, the excitable (fixed point) regime is achieved for $a > 1$ and the self-oscillating regime is achieved for $a < 1$ (stable limit cycle). The cycle appears due to supercritical Andronov–Hopf bifurcation at $a_{\mathrm{cr}} = 1$ [23].

When choosing the cell types included into the model, we follow the previously formulated principles [24,25]. Further, we also follow the notation used in [9,11], introducing brief designations for each type of cells participating in the model: cortical interneuron—IN (1 element), cortical pyramid cells—PY (4 elements), thalamocortical cells—TC (4 elements), reticular cells of thalamus—RE (4 elements), and the external input (nervus trigeminus) neuron—NT (1 element). NT neuron can excite (positive coupling, i. e. $k_{i,j} > 0$) one TC cell, TC cells excite all other types of cells except themselves and NT. PY cells can excite cells of all other types except NT, but including cells of the same type. RE cells inhibit (negative coupling, i. e., $k_{i,j} < 0$) some cells of all other types except NT, and IN cells can inhibit only PY cells. Schematic representation of one of the model coupling matrices is shown in Fig. 1.

2.2 Electrical circuit of the thalamocortical network

The principal electrical scheme of the simplified FitzHugh–Nagumo oscillator was developed in [8]; the circuit diagram of its version we used is shown in Fig. 2. The circuit contains two analog multipliers U1 and U2 and two dual operational amplifiers U3 and U4. Elements U4B and U3A are integrators, element U4A is a inverter, and element U3B is a follower. R_a is potentiometer that allow you to change the value of parameter a.

In contrast with the mathematical model, see Eq. (1), the parameters of the radioengineering circuit have dimensions. The time-scale parameters have the values $E = R_{10}C_1$ and $T = R_6C_2$. Parameter ε from (Eq.1) is calculated as $\varepsilon = E/T$. The parameter a is set by the voltage at the "+" clamp of the amplifier U3B. The total voltage drop on a series-connected resistor $R9 = 5\,\mathrm{k\Omega}$ and potentiometer $R_a = 1\,\mathrm{k\Omega}$ is $U_a = 15V$, i. e., the voltage drop on the entire potentiometer is 2.5 V. In particular, if the potentiometer is set to $A = 0\%$, the voltage 2.5 V is set to "+" input of U3B, and if the potentiometer is set to $A = 100\%$, this voltage is zero. So, the parameter a can be calculated using A measured in percents of potentiometer use as follows: $a = 2.5(1 - \frac{A}{100\%})$. It is set in volts as variables u and v actually do in the scheme (let their dimensional values be denoted as U and V). The cubic transformation is provided by the amplifiers U1 and U2. Integrators U4B and U3A allow to obtain U and V, respectively. Inverter U4A allows to obtain $-U$. Follower U3B is used for connection to the circuit of potentiometer R_a. Input $I1$ receives signal from the other neuron.

Then, an ensemble of 14 such neurons was constructed in [14] using SPICE emulator. The experimental device constructed in this paper follows the previously developed setup [14] with some minor changes reasonable due to hardware realization. It consists of 14 analog electronic circuits constructed using standard analog elements with the following nominal values: R1 = R3 = 1 kΩ, R2 = 9.1 kΩ, R4 = 2.4 kΩ, potentiometer R_a = 1 kΩ, R9 = 5 kΩ, R5 = R6 = R7 = R8 = R10 = R11 = R12 = 100 kΩ, R13–R17 determine the coupling strength k (each circuit can be linked with up to 5 others), C1 = 1 nF, C2 = 0.01 μF, U1, U2 are amplifiers of the type AD633, and U3, U4 are amplifiers of the type AD822. All generators were installed on a large sheet of one-side foil fiberglass. The individual generators were fixed to a common plate using brass PCB column and steel PCB screws, so it became possible to use the plate as a grounding for the entire installation. Bipolar power was supplied to all neurons from a common power source through a screw terminal block installed on each generator.

The principal scheme of experimental device is shown in Fig. 3. It consists of two main blocks: TCN is an ensemble of 14 FitzHugh–Nagumo circuits modeling thalamocortical system and external input, and NI PXI is a platform by National Instruments used for coupling organization and data acquisition. National Instruments PXI includes PXIe-8840 controller, with an integrated Intel Core i5-4400E dual-core processor with an operating frequency of 2.7 GHz, chassis PXIe-1075 for extension modules, multifunctional input/output modules PXIe-6361, PXIe-6355 based on parallel analogue-digital converters (ADC), digital-analogue converters (DAC), chassis for extension modules, multi-channel parallel analogue-digital converters (ADC), and digital-analogue converters (DAC).

Arrows in Fig. 3 show directions of signal propagation between blocks in the scheme. Each arrow corresponds to all channels together. The generators are connected via PXI using ADC and DAC. In particular, ADC receive signals from all nodes, the microprocessor forms the coupling terms in formula (1) using LabVIEW software and sends them to corresponding generators via DAC. So, if multiple generators drive one another, superposition of driving signals is orga-

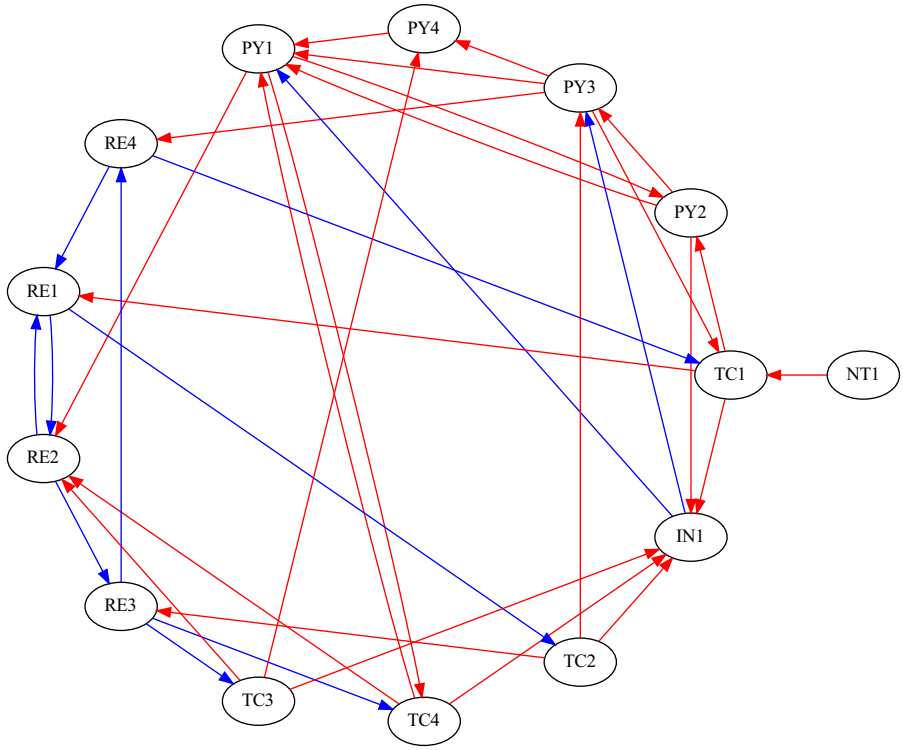

Fig. 1 Connectivity graph for the thalamocortical network with external input. Blue lines indicate negative couplings; red lines indicate positive couplings. PY—cortical pyramidal cells, IN—cortical interneuron, RE—reticular thalamic cells, NT—nervus trigeminus

nized in microprocessor in real time. Since the coupling matrix is also stored in the microprocessor, this makes the device much simpler to reset, e. g., to change couplings. The sampling frequency of ADC and DAC was equal to $f_s = 10$ kHz per channel, which was considered to be enough because the main oscillation frequency of electronic generators was about 200 Hz. The physical representation of the built circuit is shown in Fig. 4.

The parameters were mostly chosen to be near the first cycle birth bifurcation, but in the excitable (not oscillatory) regime. Such a choice provided the possibility for long transients as it was shown theoretically in the most simple two dimensional case [12]. For the mathematical model (1), the bifurcation value of parameter a is $a_{\mathrm{cr}} = 1$, if a single neuron is considered. For the electronic circuits, this value was a little bit different both due to nonideality of elements (the nonlinear cubic function in (1) was approximated imprecisely), and due to lack of element with exact nominal values, for instance, the necessary 2.2 Ω resistors were replaced by standard 2.0 Ω ones. All these factors led to a mean value $a_{\mathrm{cr}} \approx 1.057$, but it was slightly different for different generators. For the coupled generators, transition to oscillatory regime is possible for even larger values of a [11,14].

Since the generators occurred to be different by design due to nonideality of elements from which they were constructed, they were also upset by the parameter a even when the same value was expected. Further we operate with a mean for all generators (except NT) expected value of a denoted as $\overline{a}_{\mathrm{br}}$ ("br" means "brain"). For all presented further examples, this value was set equally $\overline{a}_{\mathrm{br}} = 1.2$. The coupling coefficients for all existing couplings were also set equally $k_{\mathrm{br}} = 0.05$. These values were set based on the previous consideration and bifurcation analysis of SPICE-simulated circuits done in [14,17,18] with some additional fitting to experimental device.

The external input was modeled using 14-th FitzHugh–Nagumo generator. The signal from this generator was sent to one of TC generators (in particular, TC1), as it is shown in Fig. 1. So, the coupling coefficient $k_{\mathrm{TC1,NT}}$ was responsible for the external driving. The coupling from TC was zero at first 10000 samplings of ADC (1 s). Then, the coupling was increased from 0 to 0.2

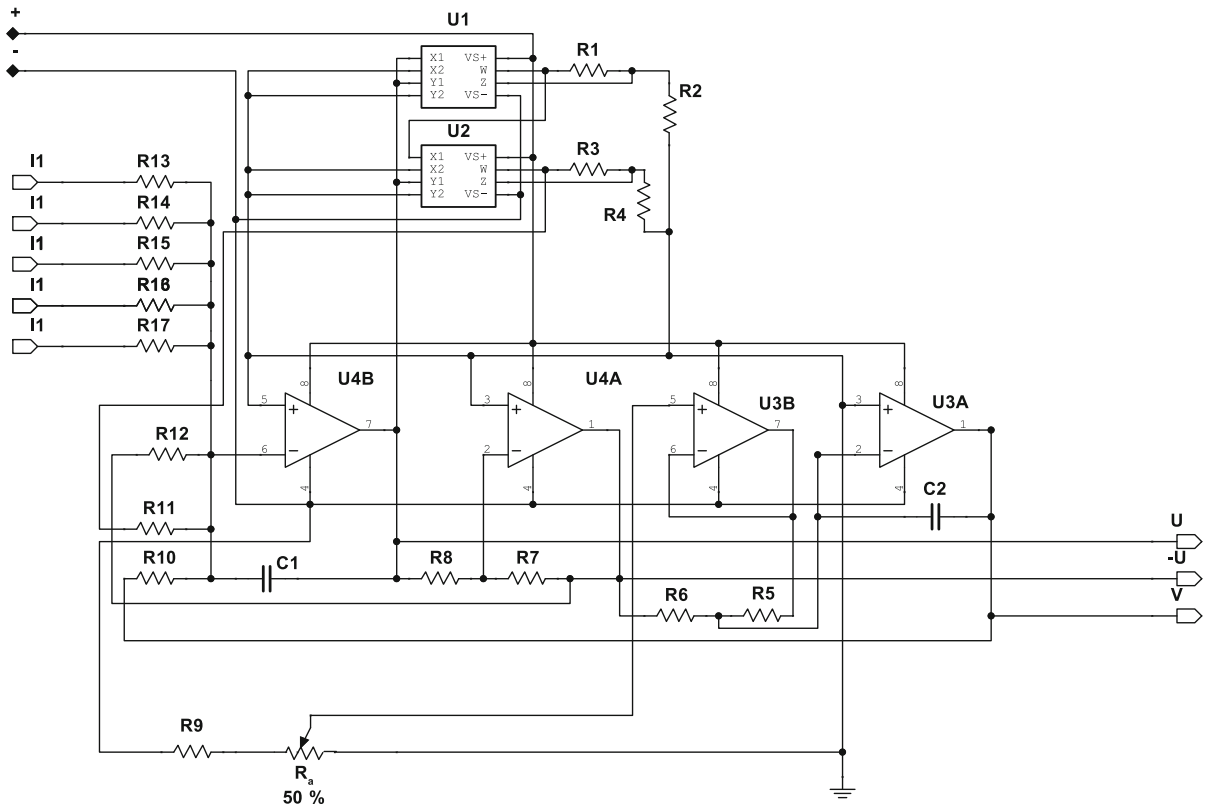

Fig. 2 Electrical circuit diagram of a single generator. R1 = R3 = 1 kΩ, R2 = 9.1 kΩ, R4 = 2.4 kΩ, potentiometer R_a = 1 kΩ, R9 = 5 kΩ, R5 = R6 = R7 = R8 = R10 = R11 = R12 = 100 kΩ, R13–R17 determine the coupling strength k, C1 = 1 nF, C2 = 0.01 μF, U1, U2 are multipliers of the type AD633, and U3, U4 are amplifiers of the type AD822

at a short time interval about 0.013–0.018 s length (we tried different duration since the dependence of regime on driving length and termination phase was shown in for both mathematical model [11] and SPICE emulator [17]), being set back to 0 after this interval finished. By itself, the NT neuron-generator was always in oscillatory mode with $a_{\mathrm{NT}} = 0.9$. To check the dependence of the duration of the discharges on the duration of the external driving w, the time moment of coupling coefficient $k_{\mathrm{TC1,NT}}$ change was set at a peak of the NT generator signal. However, such an organization had a disadvantage: since the sampling frequency of the signals is not a multiple of the main frequency of the driving signal, the slightly different phase was achieved in each new experiment.

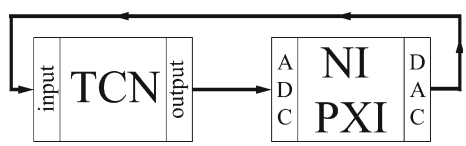

Fig. 3 Block diagram of entire electronic circuit modeling the thalamocortical network with external input. TCN is an ensemble of 14 FitzHugh–Nagumo circuits modeling thalamocortical system and external input, and NI PXI is a platform by National Instruments used for coupling organization and data acquisition

3 Results

3.1 Time–frequency characteristics

One of known scenarios of absence seizure initiation is a response to a relatively short in time sequence of pulses incoming into thalamus from peripheral external input (usually, nervus trigeminus). This sequence

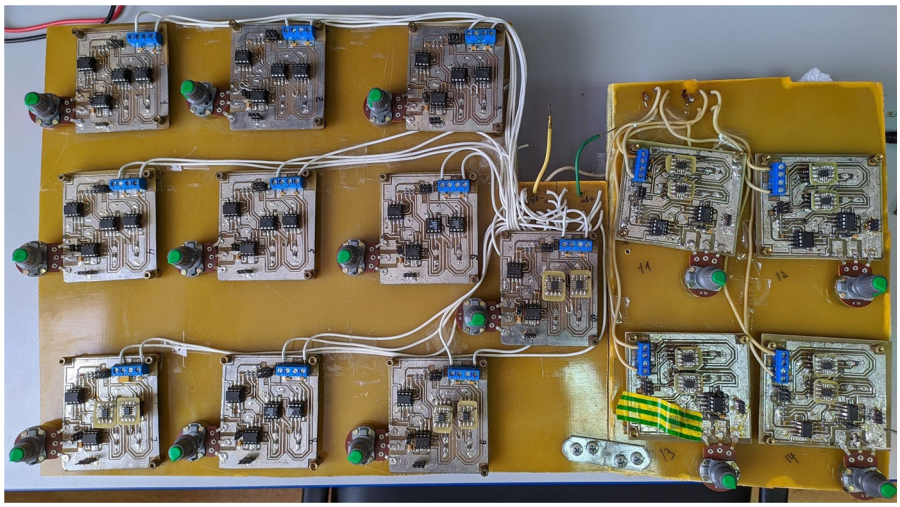

Fig. 4 Photograph of the physical representation of the built electrical circuit

starts oscillations in the network. The mechanism was known both from experiment [10] and from modeling [24,26]. In our device, the TC1 generator was a primary target of this external driving. The network switches to nonautonomous high amplitude oscillatory mode when the driving is applied. This process takes some time, as shown in Fig. 5a between to dashed vertical gray lines. The existence of the nonautonomous oscillations in the circuit is mostly trivial.

The main and most interesting outcome here is that the network continues to oscillate with approximately the same shape, frequency, and amplitude after the external driving terminates—see Fig. 5a, the oscillations to the right from the right dashed gray line. Further, we call such oscillations *residual* and denote their number as Q due to an analogy with a quality factor. Such oscillations can last much longer than nonautonomous regime, with terminating spontaneously, so they are not oscillations on some attractor. Therefore, we have to decide that short external input causes a long transient process rather than switching between two attractors: stable point and limit cycle as it was in the models [24–26]. It is typical that all cortical neurons (including the interneuron) in the setup oscillate mostly periodically in phase or with small phase shift, while thalamic neurons can be synchronized with large phase shifts, see Fig. 5a. The frequency $f_{\mathrm{br}} \sim 214$ Hz of all 13 model neurons in the thalamocortical network is the same, as it is shown in Fig. 5b, with the second harmonic being of the similar amplitude as the first one (the 3rd to 5th harmonics were also well detectable). The frequency $f_{\mathrm{NT}} \sim 224$ Hz of the external input is usually somewhat higher. The combinational harmonics with the frequencies $f_{\mathrm{br}} \pm f_{\mathrm{br}}/3$; $2f_{\mathrm{br}} \pm f_{\mathrm{br}}/3$; etc. can be seen in the spectrum of RE4 neuron in 84% of studied cases. The same combinational harmonics appear in the spectra of TC1 neuron in 53% of cases and of PY2 neuron in 16% of cases.

In biological experiments, the activity of single neurons can be recorded during absence seizures [27]. But generally, the local field potentials (LFPs) which are summary (integral) signals of relatively small brain areas, but large number of neurons ($\sim 10^4 - 10^5$) are available for measurement [28]. Most known models aim to reproduce series and spectra of LFPs [9,24–26] rather than those of single neurons. Therefore, here the integral signals of all considered brain structures were calculated by summing the signals of individual neurons and are plotted in Fig. 6a, b. In spectra of the summary signals, the main frequency is not expressed so well as it is in the spectra of individual cells; especially, large decrease was for thalamus. This takes place due to phase shift between the oscillations of thalamic neurons of the same type. However, the oscillations in model LFPs still do have a main time scale, see Fig. 6a, and the main pick with its second harmonic is still well seen, see Fig. 6b.

3.2 Variability

The brain of rats—animal models of absence epilepsy—has the approximately equal number of neurons and connections between them for each animal [29], because

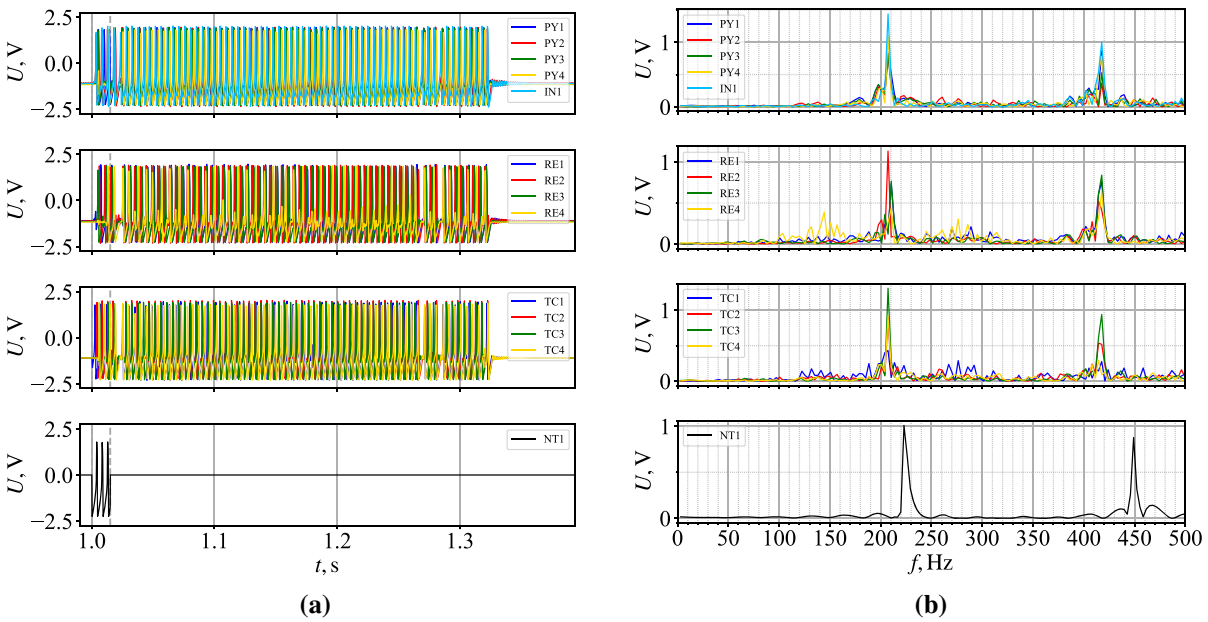

Fig. 5 Time series (**a**) and amplitude spectra (**b**) for individual neurons. PY—cortical pyramidal cells, IN—cortical interneuron, RE—reticular thalamic cells, TC—thalamocortical cells, NT—nervus trigeminus. The black lines indicate the beginning and the end of the external driving. Results are obtained at $\overline{a}_{\mathrm{br}} = 1.2$, $k_{\mathrm{br}} = 0.05$, $a_{\mathrm{NT}} = 0.9$, $k_{\mathrm{NT}} = 0.2$

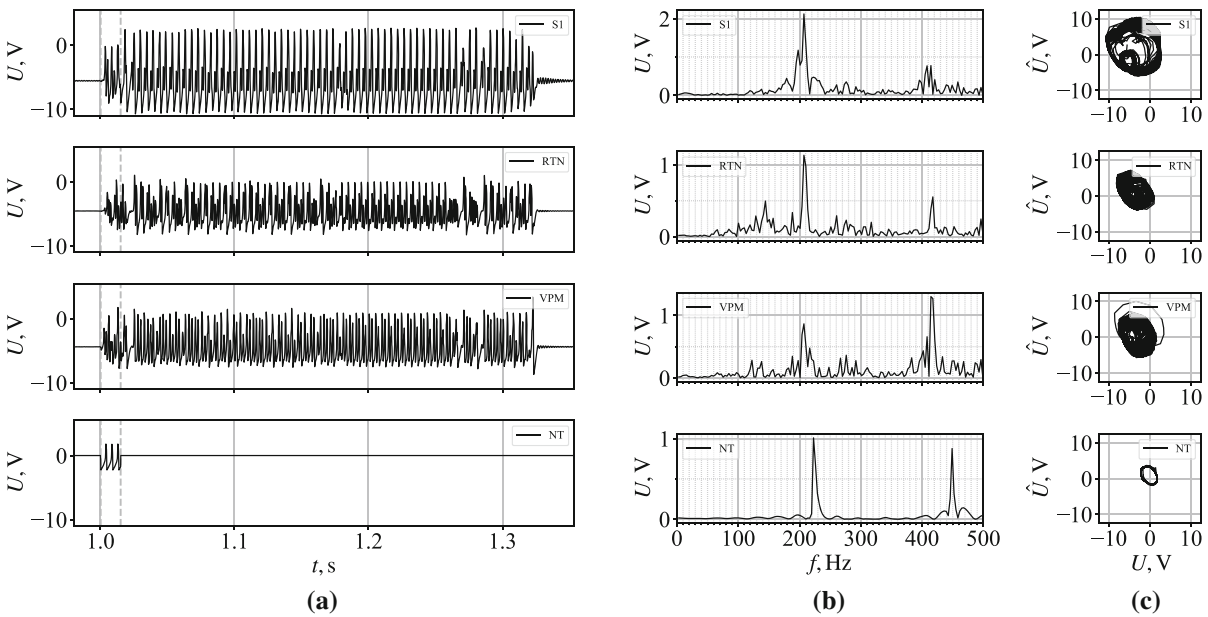

Fig. 6 Time series (**a**), amplitude spectra (**b**) and phase plots (**c**) for integral signals. The upper part is the primary somatosensory cortex (S1), which includes PY and IN cells; it is followed below by the reticular thalamic nucleus (RTN), consisting of RE-cells; the next part is the ventral posteromedial thalamic nucleus (VPM), consisting of TC-cells; the lowest part is the trigeminal neuron (NT). The black lines indicate the beginning and the end of the external driving. Results are obtained at $\overline{a}_{\mathrm{br}} = 1.2$, $k_{\mathrm{br}} = 0.05$, $a_{\mathrm{NT}} = 0.9$, $k_{\mathrm{NT}} = 0.2$

the absence epilepsy is not neurodegenerative disease [30]. At the same time, a large divergence in number and duration of SWDs over population was experimentally shown [15], as well as difference in location of involved in seizure cortical areas [31] and connectivity between them [16,32,33]. The similar diversity is also known for human patients [34]. Real epileptic seizures can largely vary their longitude: from 2 s to 12 s and more for human patients with mean length of 6 s and mean frequency ≈ 3.5 Hz [35], given averagely about 20 oscillations per seizure. For rat genetic models of GAERS and WAG/Rij strains the mean seizure length is 15 and 6 s, respectively, with main frequency about 7 Hz and 8 Hz, respectively [36], given the mean length calculated in number of oscillations equal to ~ 105 for GAERS and ~ 48 for WAG/Rij rats. The common point is that not only variability over population exists (*population variability*), but for the same animal seizures have different length (*individual variability*).

To detect how much our setup corresponds to biological phenomenon, we calculated the statistics of model SWD length, obtained in our experiments. In the device, the main frequency of residual oscillations was about 214 Hz, which is determined by details of realization including specifics of used components. Since switching to frequencies similar to those in biological experiments is impractical, and since humans and different animals have different frequency [37,38], it was decided not to try to reproduce the frequency by itself, but to reproduce a number of oscillations in a seizure (only residual oscillations were accounted). For the experiments lasting for 10 s were performed, the driving was applied in 1 s after the experiment starts. If oscillations stopped just after switching off the external driving ($Q = 0$) or oscillations did not stop at the end of experiment, such realizations were not counted into statistics.

The population variability was modeled using eight different coupling matrices with the same number of generators $D = 14$ and equal number of couplings $K = 34$: $K_+ = 23$ positive ones and $K_- = 11$ negative ones. All the matrices were constructed following the general rules formulated in [24,26] and belonged to the class proposed in [39]. To provide individual variability, i. e., to obtain different SWDs for the same coupling matrix, the different duration of external driving w was considered, setting different termination phase φ_{NT}. It should be noted that numerical experiments, in which the initial phase of the driving was varied at a fixed termination phase, have shown that the initial phase does not significantly affect the duration of the transient process, unless the driving length is minimally sufficient (about 3 oscillations or more).

In [11], the dependency of $Q(\varphi_{\mathrm{NT}})$ was shown to have well expresses periodical structure for the mathematical model. The similar, but less expressed dependency $Q(\varphi_{\mathrm{NT}})$ was shown for the simulation using SPICE software models in [17]; in particular, the longest transients were obtained for φ_{NT} at which $U_{\mathrm{NT}} \approx 0$. Here, the driving duration was varied from 3 to 4 oscillations of external driving (approximately 13.4–17.8 ms) with a step of 1/4 of oscillation length (about 1.1 ms), providing 5 different phases φ_{NT}. For each of the 8 matrices and for each of 5 driving termination phases, the experiment was performed ten times, given 400 experimental time series $U(t)$. For each series, we automatically selected a transient process, using a time point of driving termination as a beginning time point and detecting a last high amplitude pick as a final time point. For achieved transients, the Hilbert's transform was performed, providing a supplementary signal $\hat{U}(t)$. The obtained phase plots for summary signals are shown in Fig. 6c. Then, the Poincare's section by the line $U = 0$ was done, and Q was calculated automatically as number of crossing this line in the direction of increase in U. The value $U = 0$ was chosen mostly from the physiological reasons since only oscillations for which $U > 0$ are accounted as real spikes. Unfortunately, a periodic structure of $Q(\varphi_{\mathrm{NT}})$ dependency could not be reliably detected for experimental data.

To classify the obtained transients (model seizures), the bar plots of their duration were constructed, see Fig. 7. All seizures were split into four groups according to physiological views: ultrashort ($1 \leqslant Q < 8$), short ($8 \leqslant Q < 64$), long ($64 \leqslant Q < 1050$), and status ($Q \geqslant 1050$). This splitting was done according to general rules, declared in multiple physiological papers [1,2,28,40,41]. In particular, 8 oscillations are 1 s for rat models and 2.5 s for humans. Such SWDs are counted as SWDs of minimal length. 64 s is near mean/median length for WAG/Rij and GAERS animals, and seizures of larger length are usually considered as long ones.

Status epilepticus is a single seizure lasting more than 5 minutes or two or more seizures within a five-minute period without the person returning to normal behavior between them [42] ($Q = 1050$ at the frequency of 3.4 Hz). Previous definitions used a 30-

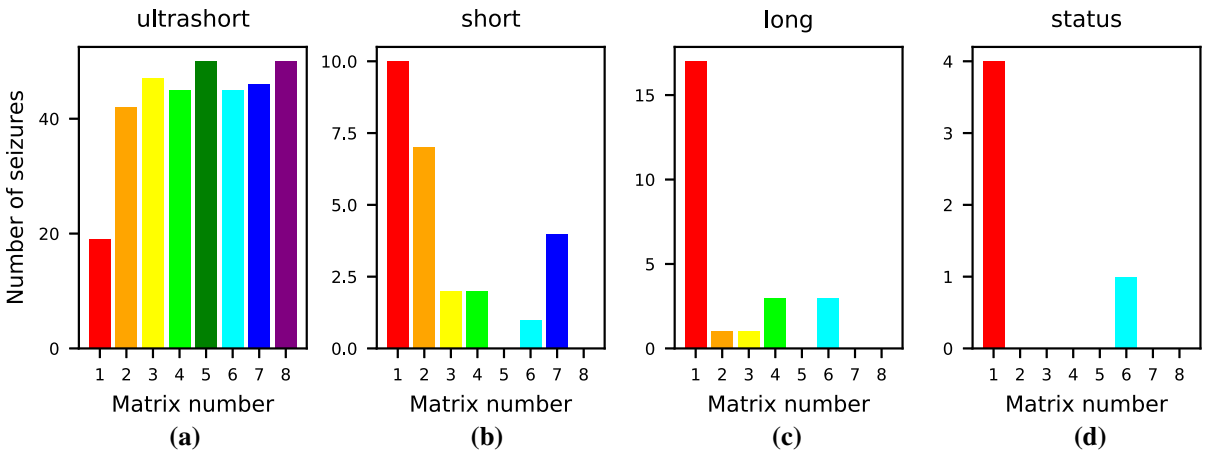

Fig. 7 Bar plots for the distribution of seizure duration. The matrix number is shown on the abscissa; number of seizures of each type for each matrix is shown on the ordinate. Seizure type: **a** ultrashort seizures are seizures with a length of less than 8 oscillations; **b** short seizures have a length from 8 to 64 oscillations; **c** long seizures have a length from 64 to 1050 oscillations; **d** status is seizures with a length of more than 1050 oscillations

minute time limit [43]. Status epilepticus occurs in up to 40 per 100,000 people per year [43]. Those with status epilepticus make up about 1% of people who visit the emergency department [42]. In our electrical model, $Q = 1050$ corresponded to 4.9 s if the main frequency was 214 Hz.

The same connectivity matrices were able to provide the transients of widely varying length. This took place not only due to different φ_{NT}, but also due to nonideality of the device, including the dependence of its characteristics on temperature. Since the observed dynamics took place near the bifurcation, when small perturbations of parameters could lead to significant changes of dynamical regime, and since all generators slightly differed one from another, such a behavior has to be considered as normal, providing a valid model for individual variability.

Though all eight matrices were of the same size and the same number of connections (24 of 34 connections were completely the same), the achieved models demonstrated different distributions of SWD length, see Fig. 7. One can see that models with matrices No. 5 and No. 8 do not demonstrate transients of appropriate duration and can be considered as models of normal activity (healthy persons or ordinary Wistar rats, from which WAG/Rij rats were obtained by selection). In opposite, the matrices No. 1 (this is matrix used in [11,14]) and No. 6 correspond to most epileptic patients with predilection to status epilepticus. The model with the matrix No. 7 can produce only short seizures similar to some animals for which the same behavior was shown [15]. The matrices No. 2–4 and 6 show both short and long seizures like typical ordinary patients or rat animal models.

4 Discussion and conclusion

In the current paper, we propose a new electronic model of neural circuit. This model is as network of 14 electronic FitzHugh–Nagumo neurons, and it is organized in accordance to modern knowledge about brain thalamocortical system. The model is able to generate long, quasiregular transient processes in response to short (3–4 pulses) driving from external input—an electronic neuron, modeling nervus trigeminus. These transients are similar to real spike-wave discharges in humans and genetic animal models (rats of WAG/Rij and GAERS strains). In particular, our circuit reproduces the following characteristics of real SWDs:

1. initiation due to an external input, as it was shown in [10] for experimental animals;
2. self-termination without any control signal or parameter change, as it was proposed in [44] based on results of coupling analysis of experimental local field potentials;

3. highly nonlinear oscillations, with the second harmonic being close to the first one, as it is for real SWDs [40];
4. close to regular, but not completely regular, synchronous oscillations of different neurons in both cortex and thalamus, with cortical oscillations being large and more synchronized, as it was multiply mentioned in literature for different animal models [1,2,28];
5. duration calculated in number of oscillations per SWD similar to experimentally measured for humans and animals;
6. variability of SWD duration for the same model (individual variability), which cannot be reproduced in mathematical model unless noise is applied;
7. population variability, i. e. different distribution of transients by length for different connectivity matrices, composed with minor rearrangement of connections and constant number of couplings, as it takes place for genetic models (population variability).

We suppose that the proposed model is rather unique among existing models of spike-wave discharges. In particular, population variability cannot be modeled in neuron-mass models like [24,25]. Individual variability cannot be naturally modeled in network mathematical models like [9] unless the noise is applied as in [26]. But if the noise is included, the bifurcation mechanisms leading to SWD generation become unclear and dynamics (especially ability to switch between regimes) becomes determined mostly by noise rather than by connectivity as in [25], while epilepsy is considered as disease caused by relatively small pathology in brain connectivity.

From the point of view of nonlinear dynamics, the model provides new and promising type of behavior—the long regular transients. The transient dynamics is of particular interest for last years in application to real world biological system modeling. It was previously observed in some mathematical models of neural networks [45,46], but only recently was considered to be suitable [47] for description of experimentally observed phenomena. Here, use of transient processes gives two significant advantages matching the properties of experimental data: first, self-termination of SWDs, and second, close to regular, but not completely periodic dynamics during the SWD. These effects are hardly to be achieved using traditional models with dynamics on the attractor. From the signal analysis point of view, the proposed system can be very useful for testing connectivity detection approaches for specificity and sensitivity, since it provides measurement procedure and individual node imperfection much closer to biological experiment than in any computational study, but allows to set connections manually, which is not possible in cell biology yet.

As a limitation of the current study, we have to notice that the proposed model is only for epileptic subnetwork of thalamocortical system, i. e., it does not produce normal activity. Normal dynamics can be also implemented if the number of generators is significantly increased, as it was demonstrated for mathematical models previously [9]. Scaling of observed dynamics by increasing number of generators in the setup was also not demonstrated here, though in mathematical models [26] and in SPICE simulation [17] it was already done. In experiment, this demands much more of hard labor because we have to construct more generators and to implement more complex, but still robust connectivity scheme. So, we hope to target this issue in future.

Acknowledgements We devote this study to the memory of professor Evgeny P. Seleznev, who left this world in September 2021. He was outstanding experimenter and has supported and inspired us for many years.

Funding This work was supported by Russian Science Foundation, Grant No. 19-72-10030.

Data availability The datasets generated during and/or analyzed during the current study are available from the corresponding author on reasonable request.

Declarations

Conflict of interest The authors declare that they have no conflict of interest.

References

1. Coenen, A.M.L., van Luijtelaar, E.L.J.M.: Genetic animal models for absence epilepsy: a review of the WAG/Rij strain of rats. Behav Genet **33**(6), 635–655 (2003). https://doi.org/10.1023/A:1026179013847
2. Marescaux, C., Vergnes, M., Depaulis, A.: Genetic absence epilepsy in rats from Strasbourg - a review. J Neur Transm Supplement (1992). https://doi.org/10.1007/978-3-7091-9206-1_4
3. Crunelli, V., Lorincz, M.L., McCafferty, C., Lambert, R.C., Leresche, N., Di Giovanni, G., David, F.: Clinical and experimental insight into pathophysiology, comorbidity and ther-

apy of absence seizures. Brain **143**(8), 2341–2368 (2020). https://doi.org/10.1093/brain/awaa072
4. Crunelli, J., Leresche, N.: Childhood absence epilepsy: genes, channels, neurons and networks. Nat. Rev. Neurosci. **3**, 371–382 (2002). https://doi.org/10.1038/nrn811
5. Destexhe, A.: Network models of absence seizures in "Neuronal Networks in Brain Function, CNS Disorders, and Therapeutics", Academic Press. (2014):11–35, https://doi.org/10.1016/B978-0-12-415804-7.00002-2
6. Thomas, A.: Memristor-based neural networks. J Phys D Appl Phys (2013). https://doi.org/10.1088/0022-3727/46/9/093001
7. Babacan, Y., Kaçar, F., Gürkan, K.: A spiking and bursting neuron circuit based on memristor. Neurocomputing (2016). https://doi.org/10.1016/j.neucom.2016.03.060
8. Kulminskiy, D.D., Ponomarenko, V.I., Prokhorov, M.D., Hramov, A.E.: Synchronization in ensembles of delay-coupled nonidentical neuronlike oscillators. Nonlin Dyn **98**(1), 735–748 (2019). https://doi.org/10.1007/s11071-019-05224-x
9. Medvedeva, T.M., Sysoeva, M.V., Lüttjohann, A., van Luijtelaar, G., Sysoev, I.V.: Dynamical mesoscale model of absence seizures in genetic models. PLoS One (2020). https://doi.org/10.1371/journal.pone.0239125
10. Abbasova, K.R., Chepurnov, S.A., Chepurnova, N.E., van Luijtelaar, G.: The role of perioral afferentation in the occurrence of spike-wave discharges in the WAG/Rij model of absence epilepsy. Brain Res **1366**, 257–262 (2010). https://doi.org/10.1016/j.brainres.2010.10.007
11. Kapustnikov, A.A., Sysoeva, M.V., Sysoev, I.V.: The modeling of spike-wave discharges in brain with small oscillatory neural networks. Math Bio Bioinfo 15(2), 138–147, (2020). https://doi.org/10.17537/2020.15.138
12. Rabinovich, M.I., Trubetskov, D.I.: Oscillat wave. In: Linear and nonlinear systems, p. 577. Kluwer Academic Publishers, Dordrecht (1989)
13. Gonchenko, A.S., Gonchenko, S.V., Kazakov, A.O., Kozlov, A., Bakhanova, Y.V. (2019) Mathematical theory of dynamical chaos and its applications: Review Part 2 Spiral chaos of three-dimensional flows Izvestiya VUZ. Appl Nonlin Dyn. https://doi.org/10.18500/0869-6632-2019-27-5-7-52
14. Egorov, N.M., Ponomarenko, V.I., Sysoev, I.V., Sysoeva, M.V.: Simulation of epileptiform activity using network of neuron-like radio technical oscillators. Techn Phys **66**(3), 505–514 (2021). https://doi.org/10.1134/S1063784221030063
15. Kalimullina, L.B., Musina, A.M., Kuznetsova, G.N.: Experimental approaches to studies of the role of the genotype at the TAG 1A locus of the dopamine D2 receptor in epileptogenesis. Neurosci Behavi Physiol **43**(8), 935–940 (2013). https://doi.org/10.1007/s11055-013-9831-z
16. Grishchenko, A.A., van Rijn, K.M., Sysoev, I.V.: Comparative analysis of methods for estimation of undirected coupling from time series of intracranial EEGs of cortex of rats-genetic models of absence epilepsy. Math Bio Bioinfor 12(2), 317–326, (2017). https://doi.org/10.17537/2017.12.317
17. Egorov, N.M., Ponomarenko, V.I., Melnikova, S.N., Sysoev, I.V., Sysoeva, M.V.: Common mechanisms of attractorless oscillatory regimes in radioengineering models of brain thalamocortical network. Izvestiya VUZ. Appl Nonlin Dyn 29(6), 927–942, (2021). https://doi.org/10.18500/0869-6632-2021-29-6-927-942
18. Egorov, NM., Ponomarenko, VI., Sysoev, IV., Sysoeva, MV.: Epileptiform activity generation by an ensemble of simplified electronic FitzHugh–Nagumo oscillators connected by a linear couplings. Proceedings of 5th Scientific School Dynamics of Complex Networks and their Applications (DCNA), (2021): 65–68, https://doi.org/10.1109/DCNA53427.2021.9586902
19. Dahlem, M.A., Hiller, G., Panchuk, A., Schöll, E.: Dynamics of delay-coupled excitable neural systems. Int J Bifurcat Chaos **19**(2), 745–753 (2009). https://doi.org/10.1142/S0218127409023111
20. FitzHugh, R.: Impulses and physiological states in theoretical models of nerve membrane. Biophys J **1**, 445–466 (1961). https://doi.org/10.1016/S0006-3495(61)86902-6
21. Nagumo, J., Arimoto, S., Yoshizawa, S.: An active pulse transmission line simulating nerve axon. Proceedings of the IRE **50**, 2061–2070 (1962). https://doi.org/10.1109/JRPROC.1962.288235
22. Binczak, S., Jacquir, S., Bilbault, J.-M., Kazantsev, V.B., Nekorkin, V.I.: Experimental study of electrical FitzHugh-Nagumo neurons with modified excitability. Neur Netwo **19**(5), 684–693 (2006). https://doi.org/10.1016/j.neunet.2005.07.011
23. Dmitrichev, A.S., Kasatkin, D.V., Klinshov, V.V., Kirillov, S.Y., Maslennikov, O.V., Shchapin, D.S., Nekorkin, V.I.: Nonlinear dynamical models of neurons: review. Izvestiya VUZ. Appl Nonlin Dyn 26(4), 5–58, (2018). https://doi.org/10.18500/0869-6632-2018-26-4-5-58
24. Suffczynski, P., Kalitzin, S., Lopes Da Silva, F.H.: Dynamics of non-convulsive epileptic phenomena modeled by a bistable neuronal network. Neuroscience. **126**(2), 467–484 (2004)
25. Taylor, P.N., Wang, Y., Goodfellow, M., Dauwels, J., Moeller, F., Stephani, U., Baier, G.: A computational study of stimulus driven epileptic seizure abatement. PLoS One (2014). https://doi.org/10.1371/journal.pone.0114316
26. Medvedeva, T.M., Sysoeva, M.V., van Luijtelaar, G., Sysoev, I.V.: Modeling spike-wave discharges by a complex network of neuronal oscillators. Neur Netw **98**, 271–282 (2018). https://doi.org/10.1016/j.neunet.2017.12.002
27. Lüttjohann, A., Pape, H.-C.: Regional specificity of corticothalamic coupling strength and directionality during waxing and waning of spike and wave discharges. Scientif Rep **9**(1), 2100 (2019). https://doi.org/10.1038/s41598-018-37985-7
28. Russo, E., Citraro, R., Constanti, A., Leo, A., Lüttjohann, A., van Luijtelaar, G., De Sarro, G.: Upholding WAG/Rij rats as a model of absence epileptogenesis: hidden mechanisms and a new theory on seizure development. Neurosci Biobehav Rev **71**, 388–408 (2016). https://doi.org/10.1016/j.neubiorev.2016.09.017
29. Paxinos, G., Watson, C.: The rat brain in stereotaxic coordinates, 6th edn., p. 456. Academic Press, San Diego (2007)
30. Berg, A.T., Berkovich, S.F., Brodie, M.J., Buchhalter, J., Cross, J.H., van Emde, Boas W., Engel, J., French, J., Glauser, T.A., Mathern, G.W., Moshe, S., Nordli, D., Plouin, P., Scheffer, I.: Revised terminology and concepts for organization of seizures and epilepsies: report of the ILAE comission on classification and terminology 2005–2010. Epilepsia (2010). https://doi.org/10.1111/j.1528-1167.2010.02522.x

31. Meeren, H.K.M., Pijn, J.P.M., van Luijtelaar, E.L.J.M., Coenen, A.M.L., Lopes da Silva, F.H.: Cortical focus drives widespread corticothalamic networks during spontaneous absence seizures in rats. J Neurosci **22**(4), 1480–1495 (2002)
32. Grishchenko, A.A., Sysoeva, M.V., Medvedeva, T.M., van Rijn, C.M., Bezruchko, B.P., Sysoev, I.V.: Comparison of approaches to directed connectivity detection in application to spike-wave discharge study. Cybernetics and Physics, (2020). https://doi.org/10.35470/2226-4116-2020-9-2-86-97
33. Martins Tenório, V.S.G., Freire, R.C.S., Santana, E.E.C., Variability of complex networks parameters on effective connectivity analysis: an absence epilepsy case.: 5th International symposium on instrumentation systems. Circuits and Transducers (INSCIT), **2021**, 1–6 (2021). https://doi.org/10.1109/INSCIT49950.2021.9557251
34. Marino, A.S., Yang, G.J., Tyrtova, E., Wu, K., Zaveri, H.P., Farooque, P., Spencer, D.D., Bandt, S.K.: Resting state connectivity in neocortical epilepsy: the epilepsy network as a patient-specific biomarker. Clin Neurophys **130**(2), 280–288 (2019). https://doi.org/10.1016/j.clinph.2018.11.016
35. Gabova, A.V., Kuznetsova, G.D., Gnezditskii, V.V., Bazyan, A.S., Obukhov, Y.V.: Method of wavelet transform in neurology: analysis of time and frequency characteristics of typical and atypical discharges of nonconvulsive epilepsy. Ann Clini Experi Neurol **3**(4), 39–44 (2009)
36. Akman, O., Demiralp, T., Ates, N., Onat, F.Y.: Electroencephalographic differences between WAG/Rij and GAERS rat models of absence epilepsy. Epilepsy Res **89**(2–3), 185–193 (2010). https://doi.org/10.1016/j.eplepsyres.2009.12.005
37. Destexhe, A.: Spike-and-wave oscillations based on the properties of GABAB receptors. J Neurosci **18**(21), 9099–9111 (1998). https://doi.org/10.1523/JNEUROSCI.18-21-09099.1998
38. Destexhe, A.: Can GABAA conductances explain the fast oscillation frequency of absence seizures in rodents? Eur J Neurosci **11**(6), 2175–2181 (1999). https://doi.org/10.1046/j.1460-9568.1999.00660.x
39. Kapustnikov, A.A., Sysoeva, M.V., Sysoev, I.V.: A class of simple networks for modeling spike-wave discharges. Proc. SPIE **11847**, 1184703 (2021). https://doi.org/10.1117/12.2589493
40. van Luijtelaar, E.L., Coenen, A.M.: Two types of electrocortical paroxysms in an inbred strain of rats. Neurosci Lett **70**, 393–397 (1986). https://doi.org/10.1016/0304-3940(86)90586-0
41. van Rijn, C.M., Gaetani, S., Santolini, I., Badura, A., Gabova, A., Fu, J., Watanabe, M., Cuomo, V., van Luijtelaar, G., Nicoletti, F., Ngomba, R.T.: WAG/Rij rats show a reduced expression of CB1 receptors in thalamic nuclei and respond to the CB1 receptor agonist, R(+)WIN55,212–2, with a reduced incidence of spike-wave discharges. Epilepsia **51**(8), 1511–1521 (2010). https://doi.org/10.1111/j.1528-1167.2009.02510.x
42. Al-Mufti, F., Claassen, J.: Neurocritical care: Status epilepticus review. Crit Care Clin **30**(4), 751–764 (2014). https://doi.org/10.1016/j.ccc.2014.06.006
43. Trinka, E., Höfler, J., Zerbs, A.: Causes of status epilepticus. Epilepsia. **53**(4), 127–138 (2012)
44. Sysoeva, M.V., Lüttjohann, A., van Luijtelaar, G., Sysoev, I.V.: Dynamics of directional coupling underlying spike-wave discharges. Neuroscience **314**, 75–89 (2016). https://doi.org/10.1016/j.neuroscience.2015.11.044
45. van Ooytien, A., van Pelt, J., Corner, M.A., Lopes da Silva, F.H.: The emergence of long-lasting transients of activity in simple neural networks. Biol Cybernet **67**, 269–277 (1992). https://doi.org/10.1007/BF00204400
46. Riecke, H., Roxin, A., Madruga, S., Solla, S.A.: Multiple attractors, long chaotic transients, and failure in small-world networks of excitable neurons. Chaos **17**(2), 026110 (2007). https://doi.org/10.1063/1.2743611
47. Afraimovich, V.S., Rabinovich, M.I., Varona, P.: Heteroclinic contours in neural ensembles and the winnerless competition principle. Int J Bifurcat Chaos **14**(04), 1195–1208 (2014). https://doi.org/10.1142/S0218127404009806